

Endocytic Trafficking of Megalin/RAP Complexes: Dissociation of the Complexes in Late Endosomes

Ralf-Peter Czekay, Robert A. Orlando, Luann Woodward,
Marita Lundstrom, and Marilyn Gist Farquhar*

Division of Cellular and Molecular Medicine, and Department of Pathology, University of California
San Diego, La Jolla, California 92093

Submitted July 1, 1996; Accepted December 13, 1996
Monitoring Editor: Ari Helenius

Megalin (gp330) is a member of the low-density lipoprotein receptor gene family. Like other members of the family, it is an endocytic receptor that binds a number of specific ligands. Megalin also binds the receptor-associated protein (RAP) that serves as an exocytic traffic chaperone and inhibits ligand binding to the receptor. To investigate the fate of megalin/RAP complexes, we bound RAP glutathione-S-transferase fusion protein (RAP-GST) to megalin at the surface of L2 yolk sac carcinoma cells and followed the trafficking of the complexes by immunofluorescence and immunogold labeling and by their distribution on Percoll gradients. We show that megalin/RAP-GST complexes, which are internalized via clathrin-coated pits, are delivered to early endosomes where they accumulate during an 18°C temperature block and colocalize with transferrin and transferrin receptor. Upon release from the temperature block, the complexes travel to late endosomes where they colocalize with rab7 and can be coprecipitated with anti-RAP-GST antibodies. Dissociation of the complex occurs in late endosomes and is most likely triggered by the low pH (~5.5) of this compartment. RAP is then rapidly delivered to lysosomes and degraded whereas megalin is recycled to the cell surface. When the ligand, lipoprotein lipase, was bound to megalin, the receptor was found to recycle through early endosomes. We conclude that in contrast to receptor/ligand complexes, megalin/RAP complexes traffic through late endosomes, which is a novelty for members of the low-density lipoprotein receptor gene family.

INTRODUCTION

Megalin (gp330) is a large endocytic receptor found in clathrin-coated pits at the apical surface of a number of epithelia (Kerjaschki and Farquhar, 1983; Kerjaschki *et al.*, 1987; Farquhar *et al.*, 1994, 1995). Megalin has been cloned (Saito *et al.*, 1994) and from its predicted protein sequence found to be a member of the low-density lipoprotein (LDL)¹ receptor gene family (Raychowdhury *et al.*, 1989), which now includes the LDL

receptor-related protein/ α_2 -macroglobulin receptor (LRP), the very low-density lipoprotein (VLDL) receptor, and the vitellogenin receptor, as well as the LDL receptor (Brown *et al.*, 1991; Krieger and Herz, 1994). Megalin, like LRP, has been shown to bind multiple ligands including apolipoprotein E-enriched β VLDL, lipoprotein lipase (LPL), urokinase/PAI-1 complexes, lactoferrin (Willnow *et al.*, 1992; Moestrup *et al.*, 1993; Kounnas *et al.*, 1994), Ca^{2+} (Christensen *et al.*, 1992), and polybasic drugs (Moestrup *et al.*, 1995). In addition, megalin binds the receptor-associated protein (RAP) (Kounnas *et al.*, 1992; Orlando *et al.*, 1992), a 44-kDa protein that blocks binding of ligands to megalin (Williams *et al.*, 1992; Willnow *et al.*, 1992; Moestrup *et al.*, 1993) and to other members of the LDL receptor family (Willnow *et al.*, 1992; Battey *et al.*, 1994; Medh *et al.*, 1995).

* Corresponding author.

¹ Abbreviations used: GST, glutathione S-transferase; LDL, low-density lipoprotein; LPL, lipoprotein lipase; LRP, LDL receptor-related protein/ α_2 -macroglobulin receptor; RAP, receptor-associated protein; RAP-GST, RAP-GST fusion protein; Tf, transferrin; TFR, transferrin receptor; VLDL, very low-density lipoprotein.

We have previously shown by coprecipitation and cosedimentation assays that RAP serves as a molecular chaperone which rapidly associates with megalin in the endoplasmic reticulum (ER; Orlando and Farquhar, 1992; Biemesderfer *et al.*, 1993; Orlando *et al.*, 1994a). Although the majority of the RAP is found in the ER (Lundstrom *et al.*, 1993; Orlando *et al.*, 1994a), in keeping with its having an ER retrieval sequence (Strickland *et al.*, 1991), it has also been detected in the Golgi (Bu *et al.*, 1994; Orlando *et al.*, 1994a; Farquhar *et al.*, 1995) and at the cell surface of several cell types [e.g., fibroblasts (Strickland *et al.*, 1991), F9 teratocarcinoma cells (Czekay *et al.*, 1995a), and glomerular epithelial cells (Kerjaschki *et al.*, 1996)]. This has led to the suggestion that RAP may function as an exocytic "traffic chaperone" for some members of the LDL receptor gene family (Bu and Rennke, 1996; Willnow *et al.*, 1996). Because RAP is an antagonist for ligand binding, its presence on the cell surface precludes uptake and internalization of ligands by megalin. For megalin to serve effectively as an endocytic receptor for its numerous ligands requires the dissociation of RAP after arrival of the megalin/RAP complex on the cell surface. The fact that the stability of megalin/RAP complexes is sensitive to low pH (Czekay *et al.*, 1995b) suggests that the complexes might dissociate in an endosomal compartment.

In this paper, we have investigated the endocytic trafficking of megalin/RAP complexes in L2 rat yolk sac carcinoma cells that express megalin and RAP (Lundstrom *et al.*, 1993; Orlando and Farquhar, 1993). Our results, obtained from immunocytochemical and cell fractionation experiments, indicate that megalin/RAP complexes traffic together through early endosomes to late endosomes where they dissociate. From there RAP is delivered to lysosomes and degraded but megalin recycles to the cell surface and is reutilized for ligand binding.

MATERIALS AND METHODS

Antibodies

Rabbit polyclonal antibodies were raised against immunoaffinity-purified megalin (Orlando and Farquhar, 1993), an 18-amino acid peptide from the C terminus of megalin (Czekay *et al.*, 1995a), and a RAP glutathione-S-transferase fusion protein (RAP-GST; Orlando and Farquhar, 1993) as described previously. Affinity-purified polyclonal IgG raised against the C terminus of rab7 was provided by Dr. Angela Wandinger-Ness (Northwestern University, Evanston, IL). Polyclonal antisera to the cytoplasmic tail of human transferrin receptor (TfR) and a mouse monoclonal antibody (mAb) directed to its extracellular domain were obtained from Dr. Ian Trowbridge (Salk Institute, La Jolla, CA). Mouse mAb to lgp120 and affinity-purified rabbit IgG against cathepsin D from rat liver were provided by Dr. Ira Mellman (Yale University School of Medicine, New Haven, CT) and Dr. Keitaro Kato (Kyushu University, Fukuoka, Japan), respectively. Mouse anti-GST mAb (catalogue number 21441) was purchased from PharMingen (San Diego, CA) and was provided by Dr. Su Huang (Ludwig Institute for Cancer Research, University of California, San Diego). Texas Red-conjugated goat

anti-rabbit and fluorescein isothiocyanate (FITC)-conjugated donkey anti-mouse Affinipure F(ab')₂ were purchased from Jackson Laboratories (West Grove, PA), and goat anti-mouse and anti-rabbit IgG gold conjugates were purchased from Amersham (Arlington Heights, IL). FITC-conjugated transferrin (FITC-Tf) was purchased from Molecular Probes (Eugene, OR).

Cell Culture

Rat L2 yolk sac carcinoma cells were grown on either coated (0.1% gelatin) plastic culture dishes (Fisher Scientific, Pittsburgh, PA) or on glass coverslips in DMEM (high glucose; UCSD Cell Culture Facility, La Jolla, CA) supplemented with 10% (vol/vol) fetal calf serum, 100 U/ml penicillin G, and 100 µg/ml streptomycin sulfate. Cells were used when ~80% confluent for immunofluorescence and as confluent monolayers for cell fractionation experiments.

Preparation of Fab Fragments of Anti-Megalyn IgG and RAP-GST

Protein A-purified anti-megalyn IgG were digested with immobilized papain, and Fab fragments were purified according to the manufacturer's instructions (Pierce, Rockford, IL). Recombinant RAP-GST was expressed and purified as described (Orlando and Farquhar, 1994b).

Internalization of RAP-GST, Anti-Megalyn Fab, and FITC-Tf

Cells were washed three times with ice-cold phosphate-buffered saline (PBS) containing 1% bovine serum albumin (BSA), pH 7.2 (PBS/BSA). RAP-GST (10 µg/ml) and FITC-Tf (200 µg/ml) were added to some cells and anti-megalyn Fab fragments (100 µg/ml) were added to others. They were then incubated for 1 h at 18°C and either 1) washed three times with ice-cold PBS/BSA or 2) washed three times in PBS/BSA at 18°C and incubated for 5 min at 37°C before being fixed and processed for immunofluorescence or immunogold labeling. Cells incubated with FITC-Tf were subsequently placed on ice, washed twice, and incubated for 5 min in ice-cold buffer A (20 mM HEPES, N-(2-hydroxyethyl)piperazine-N'-(2-ethanesulfonic acid), pH 7.4, 150 mM NaCl, 2 mM CaCl₂, pH 5.5, to release the iron from holo-Tf, after which they were incubated at 4°C in ice-cold buffer A (pH 7.2) to release apo-Tf.

Immunofluorescence and Immunogold Labeling

For immunofluorescence, L2 cells grown on glass coverslips and incubated as described above were fixed with 4% paraformaldehyde in 0.2 M phosphate buffer (pH 7.4) for 30 min, quenched with 0.05 M NH₄Cl (10 min), and permeabilized (10 min) in 0.1% Triton X-100. They were then incubated with primary rabbit and/or mouse antibodies (2 h in PBS/BSA) followed by Texas Red-conjugated goat anti-rabbit F(ab')₂ and/or FITC-conjugated donkey anti-mouse F(ab')₂ (diluted 1:200) for 1 h at room temperature and mounted in 90% glycerol/PBS containing 1 mg/ml paraphenylenediamine. Cells were examined with a Bio-Rad MRC 1000 confocal microscope equipped with a krypton-argon laser and coupled to a Zeiss Axiovert 135 M microscope as described earlier (Czekay *et al.*, 1995a). Images were processed as TIFF files by using Adobe Photoshop 3.0 software and a Power Macintosh 8500. The same software was used to create superimposed images to show overlap in the fluorescence pattern. Final images were printed on Kodak Ektatherm XLS paper with a Kodak ColorEase PS printer.

For immunogold labeling, L2 cells were fixed in 2% paraformaldehyde, 0.75 M lysine, and 10 mM sodium periodate (PLP) in phosphate buffer, pH 7.4 (McLean and Nakane, 1973), for 4 h, after which they were scraped from the dish and pelleted in a microcentrifuge. Cell pellets were cryoprotected and ultrathin cryosections were prepared as described (Hobman *et al.*, 1992; McCaffery and

Farquhar, 1995). Sections mounted on nickel grids were incubated with primary rabbit or mouse antibodies (1 h) followed by incubation (1 h) in goat anti-rabbit (5 nm gold) and/or goat anti-mouse IgG (10 nm gold) conjugates diluted 1:50 with PBS containing 10% fetal calf serum. They were then stained in 2% neutral uranyl acetate, absorption stained with 0.2% uranyl acetate in 0.2% methylcellulose and 3% polyvinyl alcohol, and examined in a JEOL 1200 EX-II electron microscope.

Radioiodination

RAP-GST, LPL, Tf, and anti-megalín Fab were radioiodinated with ^{125}I (Amersham) using Iodo-Beads (Pierce).

L2 cell surface proteins were radioiodinated with 0.3 mCi/ml in PBS at 4°C using the lactoperoxidase method as described previously (Czekay *et al.*, 1995a).

Degradation of Radioiodinated RAP-GST and Anti-Megalín Fab

L2 cells were incubated with ^{125}I -labeled RAP-GST (200 ng/ml, 21,000 cpm/ng) or ^{125}I -labeled anti-megalín Fab (200 ng/ml, 2500 cpm/ng) at 4°C for 1 h, washed, and incubation continued in DMEM (high glucose, 1 mg/ml BSA) at 37°C. Medium was collected at 0, 0.5, 1, 2, 3, and 4 h, adjusted to 15% trichloroacetic acid (TCA), incubated on ice (1 h), and microcentrifuged for 20 min at 4°C. Radioactivity in supernatants was measured in a Beckman 5500B gamma counter to determine the TCA-soluble radioactivity. The amount of ligand degraded was calculated as TCA-soluble cpm divided by the specific activity of the ligand.

Density Gradient Centrifugation

Cells were washed twice in ice-cold buffer A and harvested by scraping. Cell suspensions were centrifuged ($180 \times g$) for 5 min at 4°C. Cell pellets were resuspended in buffer A with 2 mM phenylmethylsulfonyl fluoride, forced through a 28-gauge needle (10 times), and centrifuged ($400 \times g$) for 10 min at 4°C. Postnuclear supernatants (1 ml) were top loaded onto 20% Percoll density gradients prepared by mixing 1 M Tris (pH 8, 0.15 ml), 1.5 M NaCl (1.5 ml), 100% Percoll (3 ml, Pharmacia, Alameda, CA), and double-distilled H_2O (10.35 ml). Centrifugation was carried out at 4°C in a 70.1-Ti fixed angle rotor and a Beckman L8-70 M ultracentrifuge for 50 min at $20,000 \times g$. Fractions (1 ml) were collected from the top of the gradient and analyzed by immunoprecipitation or gamma counting.

Cell Surface Binding and Uptake of ^{125}I -Labeled Tf

^{125}I -labeled Tf (200 ng/ml, 19,500 cpm/ng) in DMEM (high glucose, 1 mg/ml BSA) was bound to the cell surface of L2 cells by incubation for 30 min at 4°C. Cells were then either rinsed to remove unbound Tf and harvested by scraping or incubated for 1 h at 18°C. In the latter case, cells were rinsed at 4°C and incubated for 5 min in ice-cold buffer A, pH 5.5 (to release the iron from the holo-Tf), and 5 min in ice-cold buffer A, pH 7.2 (to release ^{125}I -labeled apo-Tf bound to cell surface receptors). Cells were then processed for cell fractionation on sucrose gradients. ^{125}I -labeled Tf present in the gradient fractions was quantitated by gamma counting.

Immunoprecipitation

Protein A-agarose beads (Bio-Rad, Hercules, CA) were washed twice with buffer A containing 0.5% Tween 20 and 1% BSA (pH 7.4). Rabbit polyclonal anti-megalín or anti-RAP-GST antiserum (5 μl) and 0.5 ml of each gradient fraction was mixed with 20 μl of beads, and the volume was adjusted to 1 ml. The mixture was incubated for 16 h at 4°C and processed for SDS-PAGE (Laemmli, 1970) as described (Czekay *et al.*, 1995). Gels were stained with 0.1% Coomassie

R in 40% MeOH, 10% acetic acid, destained, dried, and exposed to a phosphor screen for 1 to 3 days. Radioactive signals were analyzed on a Molecular Dynamics PhosphorImager using ImageQuant version 3.3 software. Alternatively, they were exposed to Kodak X-AR film at -80°C . Autoradiographs were digitized into eight-bit TIFF image files and processed as described previously (Czekay *et al.*, 1995).

Immunoblotting

Separated proteins were transferred to polyvinylidene difluoride Immobilon-P membranes (Millipore, Bedford, MA) using a semidry transfer system (MilliBlot-SDE, Millipore) at 200 mA for 40 min or a wet tank transfer system (Minigel-Transfer-Unit, Bio-Rad) at 75 mA for 16 h. Transfer membranes were blocked (30 min in PBS, pH 7.2, containing 5% calf serum and 0.1% Tween 20) followed by incubation for 2 h at room temperature with antibodies against rab7 and cathepsin D used as markers for late endosomes (Feng *et al.*, 1995) and lysosomes (Yamamoto *et al.*, 1979), respectively. Blots were then processed with the enhanced chemiluminescence detection system (Amersham, Arlington Heights, IL).

Immunoisolation of Late Endosomes

Postnuclear supernatants were fractionated on Percoll gradients as described above, and gradient fractions 6–8, shown to contain late endosomes (Figure 6), were pooled. Antibodies specific for the C terminus of megalín (Czekay *et al.*, 1995a) were prebound to protein A-agarose beads in buffer A for 2 h at room temperature. The beads were then incubated with 1 ml of the pooled fractions in buffer A for 2 h at room temperature, gently washed (five times), and incubated for 1 h on ice in buffer A containing 10 mM CHAPS, 3-[(3-chloramidopropyl)demethylammonio]-2-hydroxy-1-propanesulfonate. Samples were microfuged (2 min), and supernatants containing the solubilized proteins were centrifuged for 1 h at $100,000 \times g$ in a TL-100 ultracentrifuge, TLA-45 fixed angle rotor at 4°C (Beckman, Fullerton, CA) to pellet the Percoll. Aliquots of the final supernatants were separated by SDS-PAGE, transferred to polyvinylidene difluoride, and processed for immunoblotting with anti-rab7.

Recycling of Radioiodinated Megalín

L2 cells were surface radioiodinated as described above and incubated with RAP-GST (10 $\mu\text{g}/\text{ml}$) at 37°C for 0, 5, 10, or 20 min to allow internalization of megalín from the cell surface. Incubations were stopped by washing cells (three times) in ice-cold buffer. To assess the amount of megalín present at the cell surface, cells were incubated with anti-megalín IgG (200 $\mu\text{g}/\text{ml}$) for 2 h at 4°C, washed (three times) with ice-cold buffer A, lysed in buffer A containing 1% Triton X-100, incubated on ice for 1 h, and microcentrifuged for 10 min at 4°C. Solubilized proteins were then processed for immunoprecipitation and SDS-PAGE. We previously demonstrated that the polyclonal anti-megalín antibody used in this study remains bound to megalín under these conditions (Orlando *et al.*, 1992; Biemesderfer *et al.*, 1993).

Ligand Internalization and Degradation

L2 cells were incubated for 3 h at 37°C in the presence of ^{125}I -labeled LPL (500 ng/ml, 18,500 cpm/ng). Controls consisted of experiments in which unlabeled LPL (50 $\mu\text{g}/\text{ml}$) or unlabeled RAP-GST (50 $\mu\text{g}/\text{ml}$) was added to the incubation medium. Medium was removed after 0, 1, 2, and 3 h and microcentrifuged, and supernatants were subjected to TCA precipitation as described above and processed for gamma counting.

RESULTS

Anti-Megalin Fab and RAP-GST Are Taken Up by Endocytosis and Travel Together to Early Endosomes

The expression of megalin and RAP in L2 cells has been well documented by both immunoprecipitation (Orlando and Farquhar, 1993) and immunocytochemistry (Lundstrom *et al.*, 1993). At steady state, most of the megalin is located at the plasma membrane in clathrin-coated pits whereas the majority (~90%) of the RAP is located in the ER, with small amounts detected at the plasma membrane. To determine the fate of megalin/RAP complexes after internalization, we took advantage of the 18°C temperature block whereby endocytosed proteins accumulate in early or sorting endosomes and are prevented from progressing further down the endocytic pathway (Galloway *et al.*, 1983; Dunn *et al.*, 1989). L2 cells were incubated with anti-megalin Fab and RAP-GST in the presence of a temperature block (1 h at 18°C) or after release of the temperature block (1 h at 18°C followed by 5 min at 37°C), and their distribution was followed by immunofluorescence. RAP-GST is known to bind exclusively to megalin at the L2 cell surface (Orlando and Farquhar, 1993). After incubation for 1 h at 18°C the distribution of both anti-megalin Fab (Figure 1A) and RAP-GST (Figure 1C) overlapped with that of early endosome markers, i.e., Tf and TfR, respectively (Figure 1, B and D). These results indicate that at 18°C megalin and RAP are internalized and delivered to early endosomes. Immunogold labeling on ultrathin cryosections confirmed that anti-megalin Fab colocalized with TfR (Figure 2, A and B) on the membranes of the large endosomes characteristic of L2 cells. From these results we conclude that megalin and RAP traffic together to early endosomes where they accumulate at 18°C.

RAP but not Megalin Is Delivered to Lysosomes

To determine the fate of megalin and RAP after release of the 18°C temperature block, we next carried out incubations with anti-megalin Fab and RAP-GST at 18°C (to accumulate the complexes in early endosomes) followed by 5 min at 37°C. Upon shifting the cells to 37°C, the distribution of RAP-GST as seen by immunofluorescence (Figure 3, D and G) changed dramatically: RAP-GST no longer coincided with that of TfR (Figure 3, E and F) but instead overlapped with that of the lysosomal marker lgp120 (Figure 3, H and I). A portion of the internalized RAP-GST (Figure 3I, green dots) was found in vesicles that were significantly smaller than lysosomes and did not stain for lgp120.

The distribution of anti-megalin Fab (Figure 3A) also shifted after release of the temperature block:

although a minor fraction still overlapped with that of TfR (Figure 3B), most was found in vesicular structures that did not stain for either TfR (Figure 3C) or lgp120 (see below). Results of double immunogold labeling on ultrathin cryosections confirmed that 5 min after release of the temperature block anti-megalin Fab and TfR no longer colocalized in the same endosome (Figure 2, C and D). Even after extending the incubation at 37°C to 1 h, anti-megalin Fab was not found in structures labeled with lgp120 (Figure 4).

These results suggest that upon shifting the cells to 37°C both megalin and RAP leave early endosomes, RAP is delivered to lysosomes, and megalin travels to another endocytic compartment that does not correspond to either early endosomes or lysosomes.

RAP Is Degraded in Lysosomes

To determine whether internalized RAP is degraded or reutilized ¹²⁵I-labeled RAP-GST was bound to L2 cells at 4°C, the cells were incubated at 18°C or 37°C, and release of TCA-soluble radioactivity into the medium was determined over a 4-h period (Figure 5). When L2 cells were incubated with ¹²⁵I-labeled RAP-GST at 18°C, little TCA-soluble radioactivity was released after 4 h, whereas when cells were incubated at 37°C, TCA-soluble radioactivity was detected in the medium by 1 h and steadily increased up to 4 h. After 4 h at 37°C, 27 ng of ¹²⁵I-labeled RAP-GST were degraded. From these data and the immunofluorescence findings, we conclude that after release of the temperature block, RAP-GST is delivered to lysosomes and degraded.

By contrast when ¹²⁵I-labeled anti-megalin Fab was bound to L2 cells at 4°C and its fate was followed, there was little release of TCA-soluble radioactivity after incubation for 4 h at either at 18°C or 37°C. These results along with the immunofluorescence findings indicate that after leaving early endosomes megalin is delivered to nonlysosomal endocytic compartment and is not degraded. The questions that then arise are, Where do megalin and RAP dissociate and what is the trafficking itinerary of megalin after dissociation from RAP?

Megalin Traffics through Late Endosomes

Next we followed the distribution of internalized megalin and RAP-GST in cell fractions by using specific marker proteins to determine the location of endocytic compartments in the gradient. Postnuclear supernatants were fractionated on Percoll density gradients, and fractions were collected and immunoblotted with antibodies to TfR (early endosomes and plasma membrane), rab7 (late endosomes), and cathepsin D (lysosomes). In addition, cells were incubated with ¹²⁵I-labeled Tf at 4°C for 30 min or 4°C for 30 min followed by 18°C for 1 h to precisely locate the

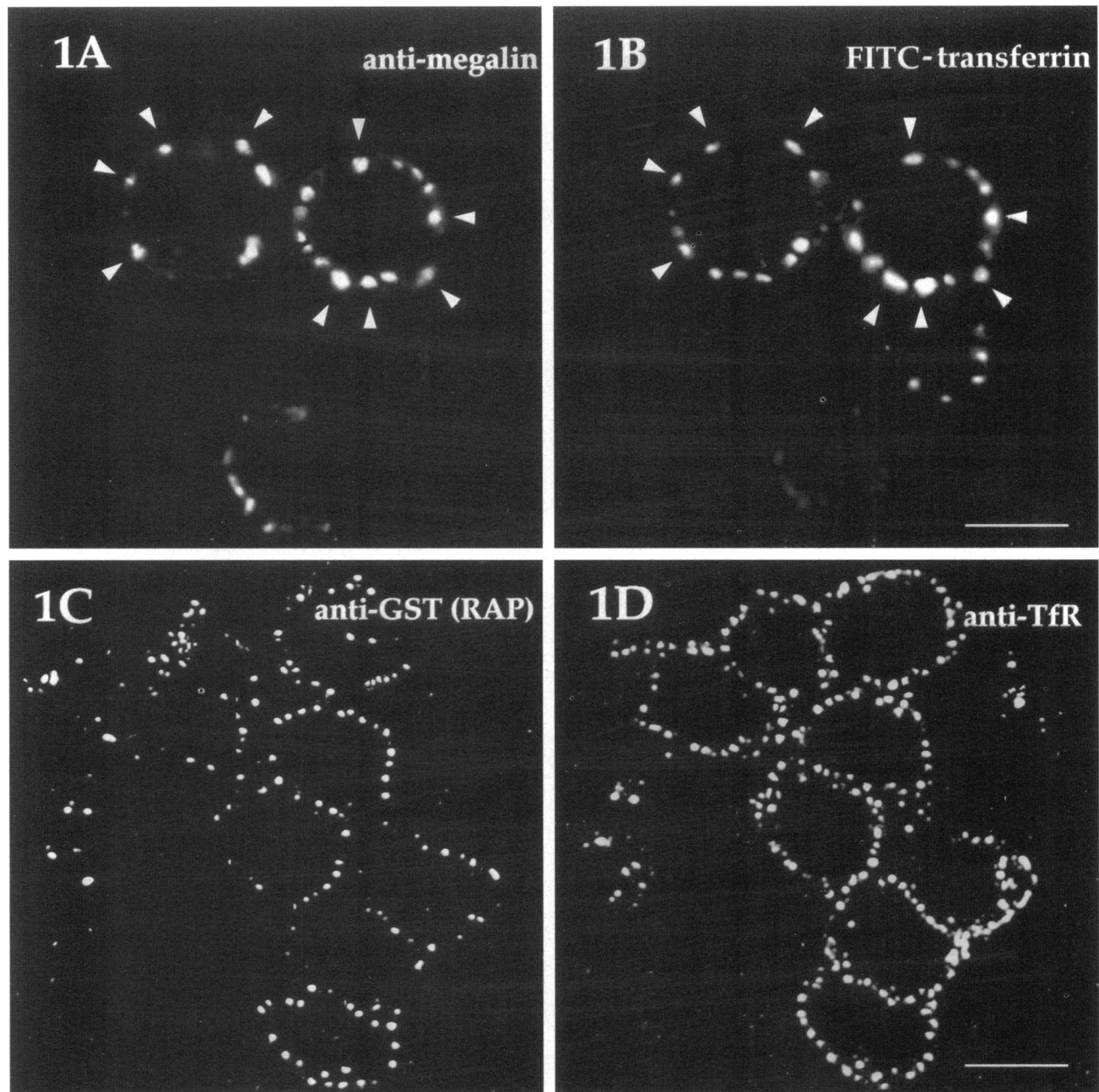


Figure 1. Anti-megalin Fab and RAP-GST colocalize with Tf and TfR after endocytosis at 18°C. Confocal images show the overlap of megalin (A) with FITC-Tf (B) as indicated by arrowheads and of RAP-GST (C) with the TfR (D). L2 cells were incubated for 1 h at 18°C with anti-megalin Fab (A) and FITC-Tf (B) or with RAP-GST alone (C), after which the cells were fixed in 4% paraformaldehyde. Cells incubated with RAP-GST were stained with polyclonal antibody against TfR (D). Internalized RAP-GST was detected with an anti-GST mAb. The location of the primary antibodies was visualized with Texas Red- or FITC-labeled secondary antibodies. Bars: A and B, 8 μm ; C and D, 10 μm .

position of plasma membrane and early endosomes in the gradient. Based on the distribution of these markers, plasma membranes were concentrated in fractions 1–3, early endosomes were concentrated in fractions 3–5, late endosomes were concentrated in fractions 6–8, and lysosomes were concentrated in fractions 10–12 (Figure 6A).

We then carried out experiments in which we followed the distribution of ^{125}I -labeled RAP-GST (bound to the cells) and megalin (labeled by cell surface iodination) in gradient fractions after incubation at 4°C, 18°C (1 h), or 18°C (1 h) followed by 37°C (5 min). After incubation at 4°C (Figure 6B, top panel), the bulk of both the megalin and RAP-GST cosedi-

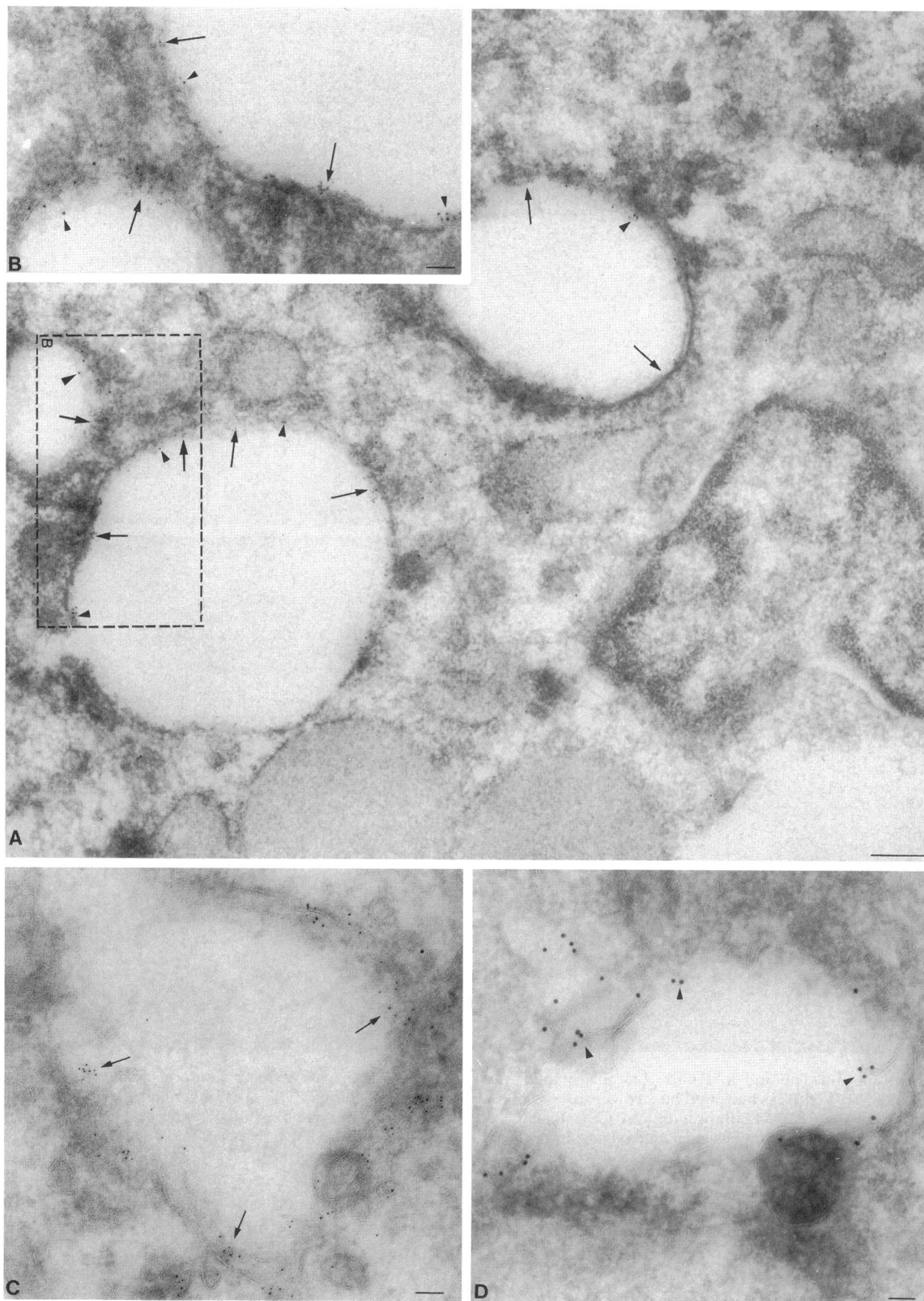


Figure 2.

mented with plasma membrane markers in fraction 2 corresponding to their expected presence on the plasma membrane. After incubation at 18°C (Figure 6B, middle panel), the peak distribution of megalin and RAP-GST shifted into the gradient and was associated with early endosomes (fractions 3 and 4). When cells were incubated at 18°C followed by 37°C (Figure 6B, bottom panel), megalin and RAP-GST shifted further into the gradient and their distributions differed. Megalin peaked in fractions 6–8 where it colocalized with the late endosome marker rab7 (Feng *et al.*, 1995), whereas RAP-GST was found predominantly in lysosomal fractions (fractions 10–12). These results suggest that 1) megalin and RAP traffic together to early endosomes; 2) within 5 min after release of the temperature block, megalin and RAP leave early endosomes and dissociate; and 3) the bulk of the RAP rapidly traffics to lysosomes whereas megalin accumulates in a compartment that cosediments with late endosomes.

Megalyn and rab7 Are Present in the Same Compartment

Next we used immunoisolation to investigate whether the megalin and rab7 that cosediment after release of the temperature block are present within the same endosomes. Toward this end, we incubated L2 cells with RAP-GST and carried out cell fractionation as described above. Fractions 6–8 containing rab7 were pooled, and vesicles that contained megalin were immunoisolated by incubation with antibodies that recognize the cytoplasmic tail of megalin precoupled to protein A-agarose beads. Immunoisolated vesicles were then processed for immunoblotting with anti-rab7 IgG.

After a 1-h incubation at 18°C (Figure 7, lane 1), little or no rab7 was detected in the vesicles immunoisolated on anti-megalyn beads. However, after shifting the cells to 37°C for only 5 min (Figure 7, lane 2), rab7 was detected in the immunoisolated fractions. These results provide direct evidence that 5 min after release of the temperature block, megalin and rab7 are found in the same late endosome compartment.

Figure 2 (cont). Megalin leaves early endosomes after release of the 18°C block. L2 cells were incubated with anti-megalyn Fab for 1 h at 18°C (A and B) or for 1 h at 18°C followed by 5 min at 37°C (C and D) and processed for immunogold labeling as described in MATERIALS AND METHODS. Ultrathin cryosections were incubated with goat anti-rabbit IgG coupled to 5 nm of gold (to detect the distribution of anti-megalyn Fab) and with anti-TfR mAb followed by goat anti-mouse IgG coupled to 10 nm gold. (A) After incubation at 18°C, megalin (arrows) and TfR (arrowheads) are localized in the same endosomes. (B) Enlargement of the boxed area in A. (C and D) After shifting the cells to 37°C for 5 min, megalin (arrows) and TfR (arrowheads) no longer colocalize and are found in different endosomes. Bar, 0.5 μ m.

Megalyn/RAP Complexes Are Found in Late Endosomes

The question then arises as to where megalyn/RAP complexes dissociate. To investigate this question, L2 cells were radioiodinated and 125 I-labeled RAP-GST was bound to the cell surface for 30 min at 4°C. Cells were then incubated and processed for cell fractionation as before. Proteins from each fraction were solubilized and immunoprecipitated either with anti-RAP-GST antibodies under conditions known to coprecipitate megalyn (Orlando *et al.*, 1992) or with anti-megalyn antibodies.

After incubation for 1 h at 18°C (Figure 8A, top panel), the majority of the megalyn that coprecipitated with RAP-GST was found in early endosomes (fractions 3–5). After release of the temperature block (5 min at 37°C), nearly one-half (46%) of the total megalyn that coprecipitated with RAP-GST (Figure 8A, middle panel) was found in late endosome fractions (6–8). After 10 min at 37°C (Figure 8A, bottom panel), the amount of megalyn coprecipitated with RAP-GST from late endosomes (fractions 6–8) was greatly decreased and was barely detectable. However, if megalyn was immunoprecipitated from these fractions with anti-megalyn antibodies (Figure 8B), a significant amount of megalyn could still be found in late endosomes (fractions 6–8). Taken together, these results suggest that endocytosed megalyn/RAP complexes leave early endosomes and travel as a complex to late endosomes where they dissociate.

Megalyn Recycles to the Cell Surface

We next investigated whether megalyn recycles to the cell surface after dissociation of RAP. Toward this end, L2 cells were surface radioiodinated at 4°C, and RAP-GST was bound to the cells to promote internalization of the receptor. The cells were incubated at 37°C for 0 to 20 min, after which the amount of 125 I-labeled megalyn at the cell surface was determined by immunoprecipitation (Figure 9). The amount present at the cell surface at 4°C (100%) was compared with that after 5, 10, or 20 min of incubation. After 5 min at 37°C only 30% of the radiolabeled megalyn remained at the cell surface, indicating that ~70% of the megalyn had been internalized. After 10 min the amount of megalyn at the cell surface increased to 50% and at 20 min to ~80%, indicating that most of the internalized receptors recycle to the plasma membrane within 20 min. These data demonstrate that after internalization of megalyn/RAP complexes and their dissociation, megalyn is rapidly recycled to the cell surface.

Megalyn/LPL Complexes Dissociate in Early Endosomes

We next wondered whether the trafficking itinerary of megalyn with bound ligand is the same as that of

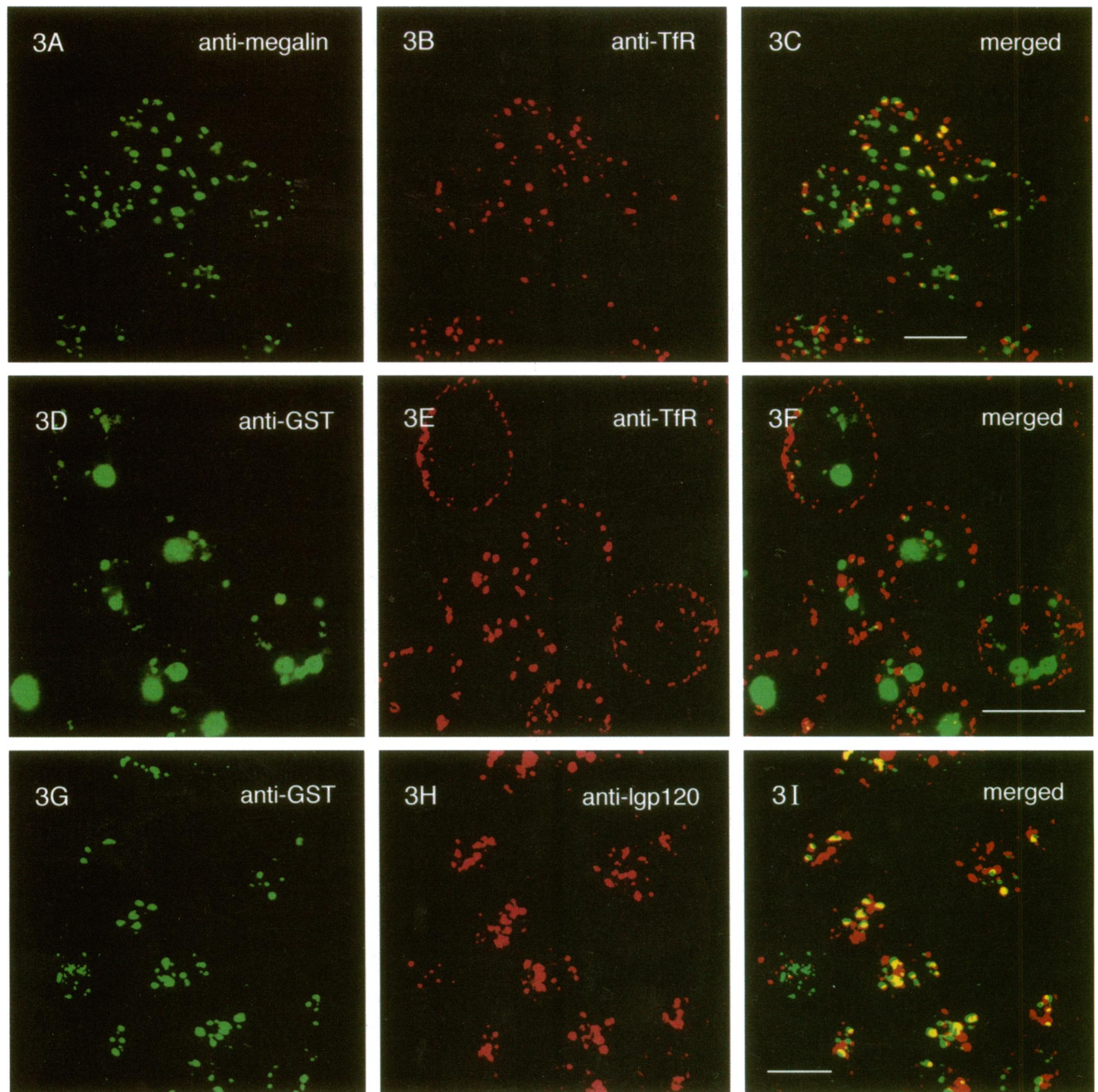


Figure 3. RAP-GST traffics to lysosomes after release of the temperature block. L2 cells were incubated with anti-megalin Fab or RAP-GST for 1 h at 18°C, after which they were shifted to 37°C for 5 min. Cells were processed for immunofluorescence and confocal microscopy as in Figure 1. Confocal images show that 5 min after removal of the temperature block, RAP-GST (D) no longer colocalizes with TfR (E and F). The majority of the RAP-GST (G) colocalizes with the lysosomal marker Igp120 (H), suggesting that RAP-GST is present in lysosomes. The majority of the anti-megalin Fab (A) no longer overlaps significantly with the TfR (B and C). A few of the endosomes (C, yellow dots) are doubly stained for megalin and TfR. Bar, 10 μ m.

megalin with bound RAP. To answer this question, we studied the uptake of 125 I-labeled LPL by L2 cells. First, cells were incubated for 3 h at 37°C with either 125 I-labeled LPL alone or in the presence of unlabeled

LPL and unlabeled RAP-GST. Addition of either unlabeled LPL or RAP-GST decreased degradation of 125 I-labeled LPL by $\sim 90\%$ (Figure 10A), indicating binding was specific. Since RAP binds exclusively to

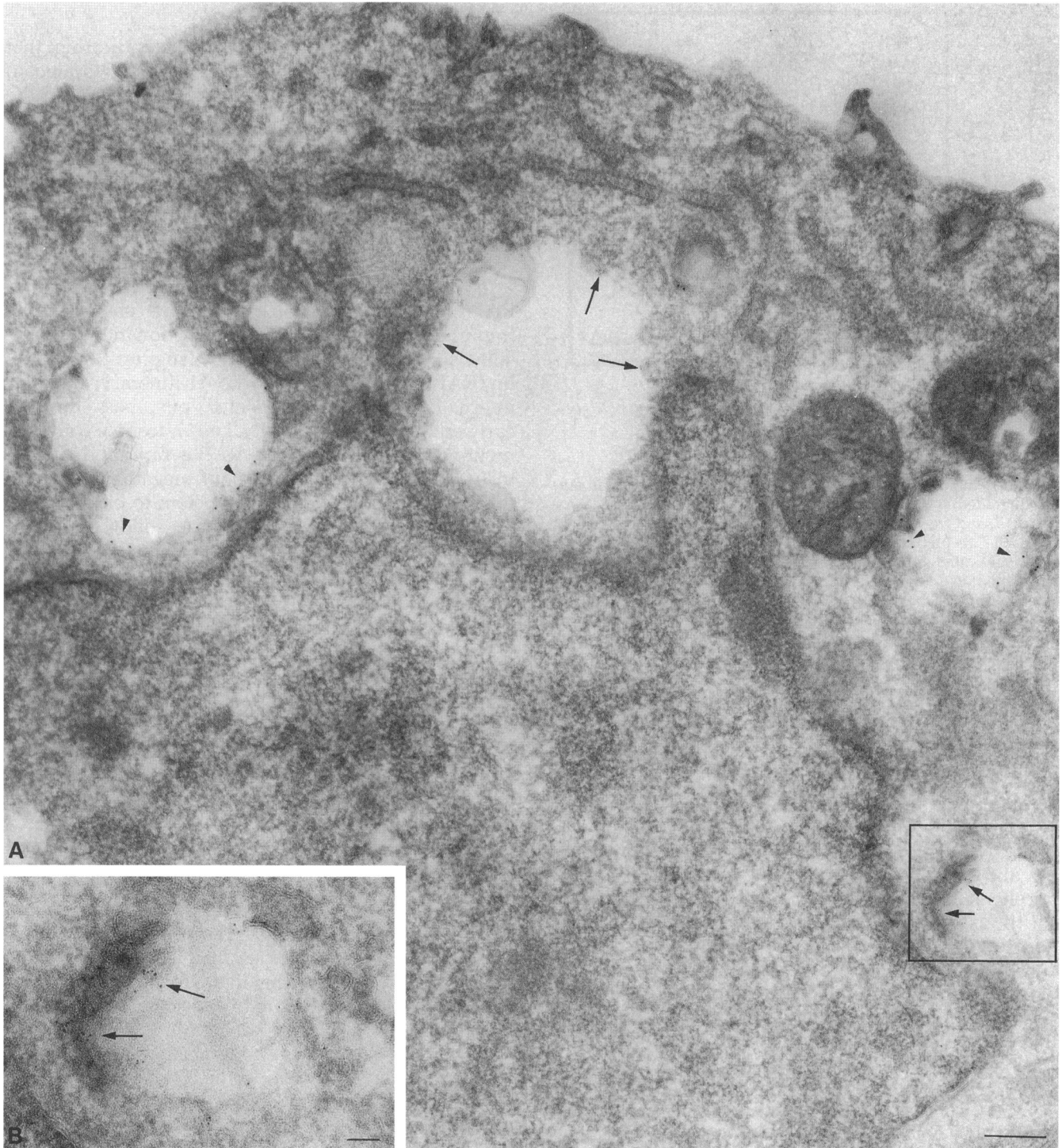


Figure 4. (A) Anti-megalin Fab is not found in lysosomes. L2 cells were incubated for 1 h at 37°C with anti-megalin Fab and processed for immunogold labeling as in Figure 2. Ultrathin cryosections were incubated with anti-Igp120 mAb. Anti-megalin Fab was detected with goat anti-rabbit IgG (5 nm gold, arrows), and anti-Igp120 was detected with goat anti-mouse IgG (10 nm gold, arrowheads). Even after extending the incubation to 1 h, there was no colocalization between anti-megalin Fab and Igp120. (B) Enlargement of boxed area in A to show small (5 nm) gold. Bar, 0.5 μ m.

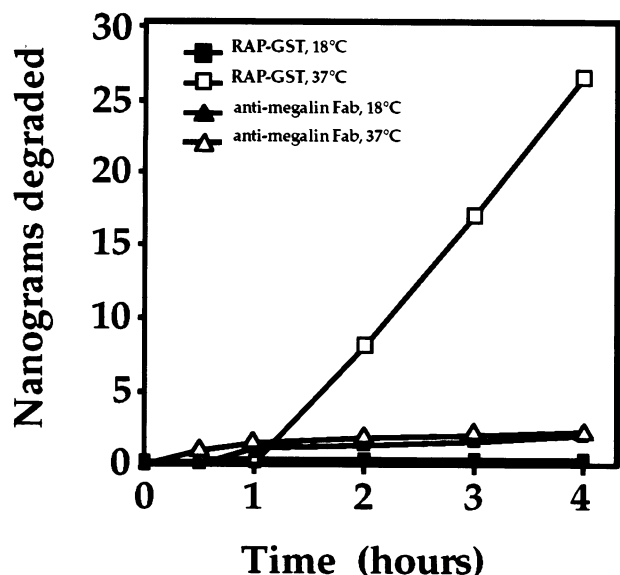


Figure 5. Internalized RAP-GST but not anti-megalin Fab is rapidly degraded at 37°C. L2 cells were incubated at 18°C or 37°C for 4 h in serum-free DMEM in the presence of either ^{125}I -labeled RAP-GST (200 ng/ml) or ^{125}I -labeled anti-megalin Fab (200 ng/ml). At the indicated times, release of TCA-soluble radioactivity was determined by gamma counting of the culture medium. After incubation with ^{125}I -labeled RAP-GST, significant release of TCA-soluble radioactivity was detected over 4 h at 37°C (□) but not at 18°C (■). Twenty-seven nanograms of ^{125}I -labeled RAP-GST were degraded over 4 h. After incubation with ^{125}I -labeled anti-megalin Fab, little TCA-soluble radioactivity was detected in the medium up to 4 h at either 37°C (△) or 18°C (▲).

megalin at the cell surface of L2 cells (Orlando and Farquhar, 1993), the fact that RAP competes for binding demonstrates that internalization of LPL occurs specifically via megalin.

Next we followed the distribution of ^{125}I -labeled LPL and ^{125}I -labeled megalin (Figure 10, B–D) labeled by cell surface iodination on Percoll density gradients exactly as for ^{125}I -labeled RAP-GST and ^{125}I -labeled megalin (see Figure 6). After internalization for 1 h at 18°C, the majority of the ^{125}I -labeled LPL (Figure 10B) and megalin (our unpublished results) was detected in fractions 1–4, indicating their presence, as expected, at the plasma membrane and in early endosomes. After shifting the temperature to 37°C for 5 min, most of the ^{125}I -labeled LPL cosedimented with cathepsin D in fractions 10–12 (Figure 10B), indicating that most of the ligand had reached lysosomes. Some (18%) of the total detectable ^{125}I -labeled LPL cosedimented with late endosomes (fractions 6–8). By contrast, the majority of the megalin (Figure 10, C and D) was precipitated from early endosomes (fractions 3–4).

Thus, these data suggest that after internalization of megalin/LPL complexes megalin traffics to early endosomes and, in contrast to megalin/RAP complexes, does not reach late endosomes.

DISCUSSION

We have previously presented data indicating that megalin, a multiligand endocytic receptor located in clathrin-coated pits, binds its chaperone, RAP, in the ER and megalin/RAP complexes can be detected at the cell surface (Biemesderfer *et al.*, 1993; Orlando and Farquhar, 1993). For megalin to function in ligand uptake at the cell surface, it must be free of bound RAP because RAP reduces or prevents binding of all known ligands to megalin (Willnow *et al.*, 1992; Kounnas *et al.*, 1993; Moestrup *et al.*, 1993).

In this report, we investigated the fate of megalin/RAP complexes internalized from the cell surface by immunocytochemistry and cell fractionation. The results, summarized in Figure 11A, suggest that megalin/RAP complexes have a novel itinerary: they are internalized via clathrin-coated pits, pass through early endosomes, and reach a late endosome compartment where they dissociate. RAP is rapidly delivered to lysosomes and degraded, but megalin recycles to the cell surface where it is competent to bind ligand.

Initially megalin/RAP complexes follow the same route as many other receptor/ligand complexes: they are internalized via clathrin-coated pits and delivered to early or sorting endosomes. Their presence in early endosomes was demonstrated by colocalization with TfR and FITC-Tf by immunofluorescence and by their cosedimentation with TfR and ^{125}I -labeled Tf in Percoll density gradients after an 18°C temperature block. The trafficking of RAP-GST was followed after binding iodinated RAP to the cell surface, and the trafficking of megalin was followed by both iodination of cell surface megalin and by tagging megalin with anti-megalin Fab. Our data further indicate that after release of the temperature block, the complexes travel together to a late endosome compartment where they dissociate. That megalin reaches late endosomes was suggested by the finding that the bulk of the megalin cosediments with the small GTP-binding protein rab7, a marker for late endosomes, and was unequivocally demonstrated by showing that vesicles immunoprecipitated on anti-megalin coated beads contained rab7 by immunoblotting. The fact that by immunofluorescence megalin was found in a compartment that did not contain either early endosome (TfR) or lysosome (lgp120) markers was in keeping with the biochemical findings. We were unable to check for the presence of rab7 by immunofluorescence due to lack of a suitable antibody. The conclusion that megalin and RAP traffic together to late endosomes is based on the finding that megalin/RAP-GST could be precipitated with anti-RAP-GST from a fraction enriched in late endosomes. The possibility that the complexes were formed artificially after solubilization could be ruled out because it was established earlier that under the conditions used,

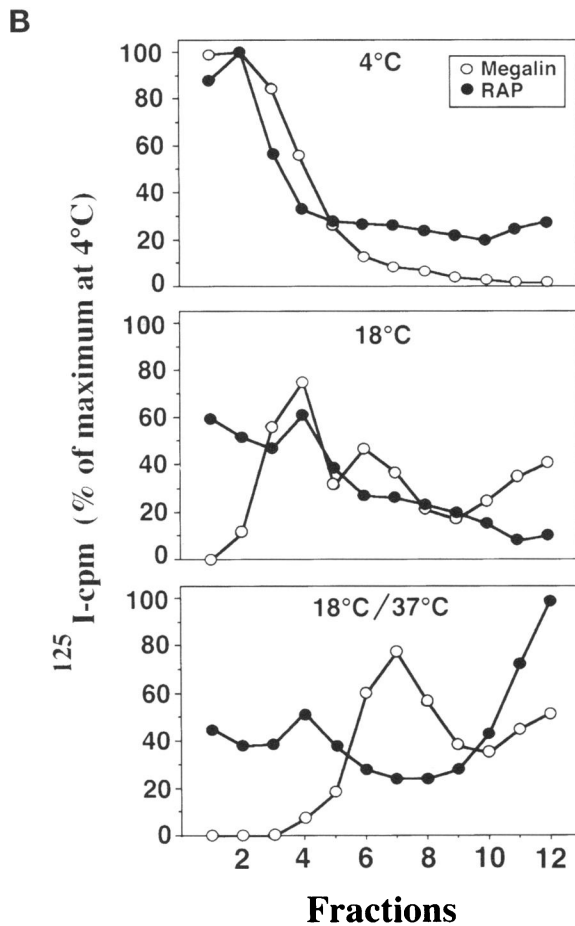
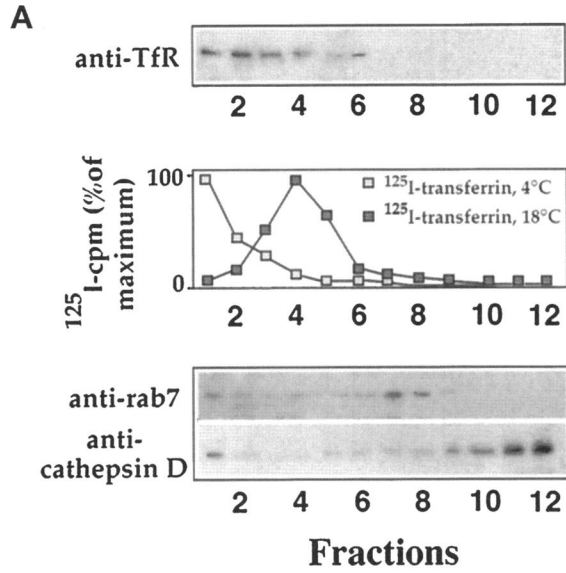


Figure 6. Megalin traffics to late endosomes. L2 cells were surface iodinated and incubated with ¹²⁵I-labeled RAP-GST at 4°C or 18°C for 1 h or for 1 h at 18°C followed by 5 min at 37°C. Postnuclear supernatants were fractionated on Percoll density gradients, and fractions were processed for immunoblotting of marker proteins, immunoprecipitation of ¹²⁵I-labeled megalin (after cell surface

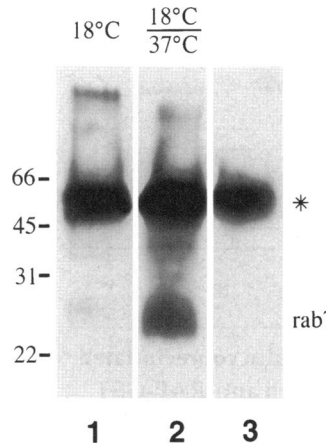


Figure 7. Immunoisolation of late endosomes. L2 cells were incubated with unlabeled RAP-GST at 18°C for 1 h (lane 1) or at 18°C for 1 h followed by 37°C for 5 min (lane 2), and postnuclear supernatants were fractionated on Percoll density gradients as in Figure 6. Fractions 6–8 containing late endosomes were pooled and incubated with antibodies against the C terminus of megalin prebound to protein A-agarose beads. The immunisolated endosomes were solubilized, and the presence of rab7 was assessed by immunoblotting using the enhanced chemiluminescence

detection system. After incubation at 18°C (lane 1), little or no rab7 is detected in the immunisolated fraction, but after release of the temperature block (lane 2), rab7 is readily detected in endosomes immunisolated on anti-megalyn-coated beads. Lane 3 is a control experiment in which no cell fractions were present during the immunoisolation. The asterisk indicates the location of the heavy chain of rabbit anti-megalyn IgG.

solubilized megalin and RAP cannot reassociate (Orlando and Farquhar, 1993).

It was surprising that only 5 min after release of the temperature block, the majority of the RAP-GST was already found in lysosomes based on colocalization by immunofluorescence and cosedimentation on Percoll gradients. This suggests that megalin/RAP complexes dissociate upon arrival in late endosomes, and RAP is rapidly transferred to lysosomes. That degradation of RAP but not megalin takes place in lysosomes was shown by the presence of TCA-soluble radioactivity in the culture medium after uptake of ¹²⁵I-labeled RAP-GST but not after endocytosis of ¹²⁵I-labeled anti-megalyn Fab. Megalin is rapidly (within 20 min after uptake) recycled to the cell surface.

Further evidence supporting a model whereby megalin and RAP dissociate in late endosomes comes

(**Figure 6 cont.** iodination), or direct gamma counting of ¹²⁵I-labeled RAP-GST and ¹²⁵I-labeled Tf as described in MATERIALS AND METHODS. (A) Distribution of compartment markers. Top, TfR is found in fractions 1–5. Middle, ¹²⁵I-labeled Tf bound at 4°C, used as a marker for plasma membrane, is concentrated in fractions 1–3 (□). ¹²⁵I-labeled Tf internalized for 1 h at 18°C, used as a marker for early endosomes, peaks in fractions 3–5 (■). Bottom, rab7, a late endosome marker, is found in fractions 6–8, and cathepsin D, a lysosome marker, is in fractions 10–12. (B) Top, when cells are incubated at 4°C, ¹²⁵I-labeled megalin and ¹²⁵I-labeled RAP-GST cosediment with ¹²⁵I-labeled Tf in fractions 1 and 2. Middle, after 1 h at 18°C, the major peaks of both megalin and RAP-GST cosediment with ¹²⁵I-labeled Tf in early endosomes (fractions 3 and 4). Bottom, after shifting the temperature to 37°C, the majority of the megalin peaks in late endosomes (fractions 6–8) cosedimenting with rab7. The majority of ¹²⁵I-labeled RAP-GST is found in lysosomal fractions (fractions 10–12) cosedimenting with cathepsin D.

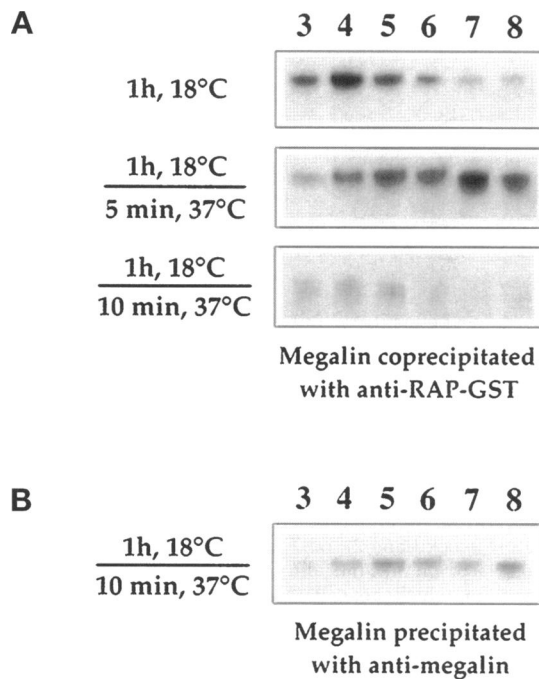


Figure 8. Megalin/RAP complexes are present in late endosomes. ^{125}I -labeled RAP-GST was bound to surface iodinated L2 cells at 4°C, after which the cells were incubated at 18°C (1 h) or at 18°C followed by 37°C for 5 or 10 min. Cell fractions were prepared as in Figure 6. Immunoprecipitation was carried out either with anti-RAP-GST (A) under conditions known to coprecipitate megalin or with anti-megalin (B) antibodies. (A) After incubation at 18°C (top), most of the megalin coprecipitated from L2 cell fractions with anti-RAP-GST is found in fractions 3–5 (early endosomes). After release of the temperature block by incubation of cells for 5 min at 37°C (middle), the majority of the coprecipitated megalin is found in fractions 6–8 (late endosomes). After a 10-min incubation at 37°C (bottom), very little megalin can be coprecipitated from late endosomes (fractions 6–8) with anti-RAP-GST. (B) Megalin can be directly precipitated with anti-megalin antibodies from fractions 6–8 after a 10-min incubation at 37°C, suggesting that a small amount of megalin is present in late endosome fractions, but it is not bound to RAP.

from the pH sensitivity of megalin/RAP complexes. We previously showed (Czekay *et al.*, 1995b) that the binding of RAP-GST to megalin is pH sensitive, and 50% of the binding was inhibited at pH 5.5, a pH typical of that of late endosomes (Yamashiro and Maxfield, 1984).

Interestingly, we found that the trafficking itinerary of megalin with bound LPL, a well-studied ligand taken up by megalin (Willnow *et al.*, 1992; Kounnas *et al.*, 1993), is different from that of megalin/RAP-GST complexes (Figure 11B): After release of the temperature block megalin cosedimented in early endosomes with TfR. Thus, after ligand binding megalin, like the LDL receptor (Goldstein *et al.*, 1985), appears to recycle through early rather than late endosomes.

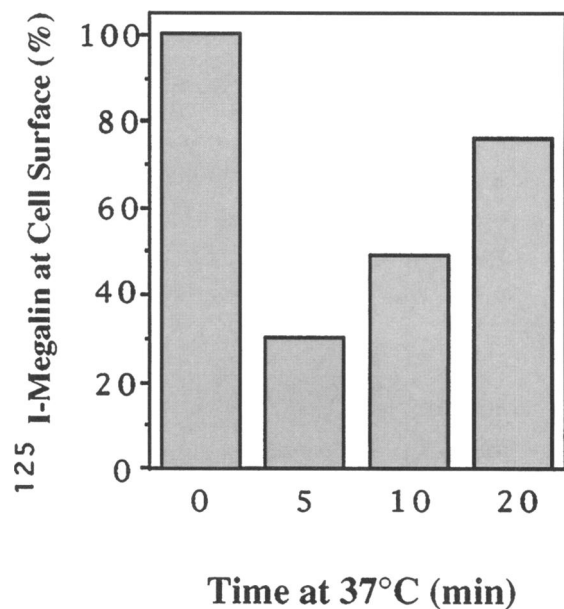


Figure 9. Megalin recycles to the cell surface after dissociation of RAP. L2 cells were surface iodinated, and RAP-GST was bound to the cells at 4°C as in Figure 6. Cells were incubated at 37°C for 0, 5, 10, or 20 min, and the amount of ^{125}I -labeled megalin at the cell surface was quantitated by cell surface immunoprecipitation and PhosphorImager analysis. After incubation for 5 min at 37°C, only 30% of the total radioiodinated megalin bound to the cells at 4°C (0 min) can be detected on the cell surface, indicating that 70% of the receptor has been internalized. At 10 min (50%) and 20 min (80%), increasing amounts of megalin are precipitated from the cell surface, indicating that two-thirds of the internalized megalin recycles to the plasma membrane within 20 min after internalization. Each value represents the average of duplicates and values differed by <10%.

Few Receptors Recycle from Late Endosomes

There are two common itineraries taken by endocytic receptors (Goldstein *et al.*, 1985; Trowbridge *et al.*, 1993; Lamaze and Schmid, 1995): One, followed by recycling receptors such as LDL, TfR, and asialoglycoprotein receptors, involves delivery of receptor/ligand complexes to early or sorting endosomes where the two dissociate and the ligand is delivered to lysosomes, whereas the receptor is sorted and returned to the cell surface (Trowbridge *et al.*, 1993). The pathway of these receptors is the same regardless of whether occupied or not. Another variant is represented by epidermal growth factor and other growth factor receptors (Lamaze and Schmid, 1995). When unoccupied these receptors recycle through early endosomes, but after ligand binding the receptor is down-regulated, i.e., both the receptor and ligand are targeted to lysosomes and degraded. Thus, the recycling of receptors through late endosomes is a novelty for endocytic receptors, especially among members of the LDL receptor gene family.

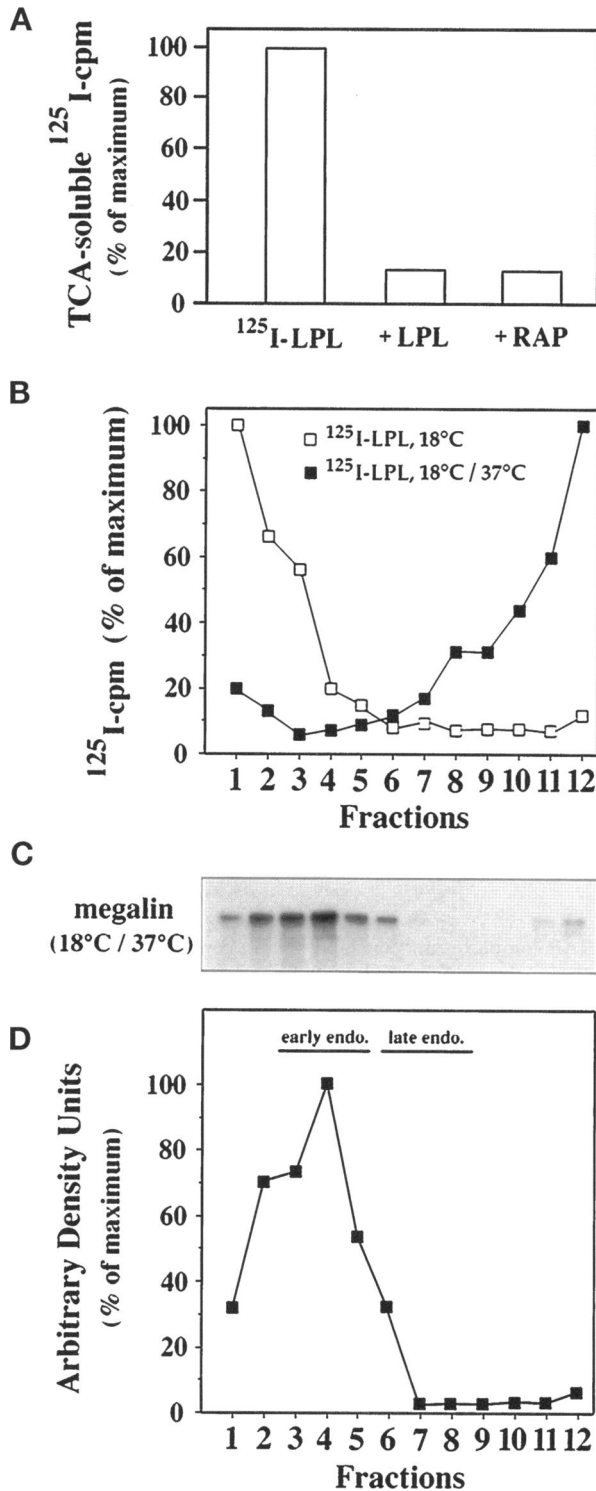


Figure 10. Megalin/LPL complexes dissociate in early endosomes. (A) Cell surface-labeled L2 cells were incubated with ¹²⁵I-labeled LPL (500 ng/ml) alone or in the presence of unlabeled LPL or unlabeled RAP-GST for 3 h at 37°C, and release of TCA-soluble radioactivity into the medium was assessed as in Figure 5. The presence of LPL and RAP-GST decreased the degradation of

The only receptor known to recycle from late endosomes (sometimes also referred to as prelysosomes) is the mannose-6-phosphate receptor, which functions to transport lysosomal enzymes from the trans Golgi network (TGN) to lysosomes (Duncan and Kornfeld, 1988; Kornfeld and Mellman, 1989). It does so by delivering its cargo and recycling primarily from late endosomes (Brown *et al.*, 1986; Griffiths *et al.*, 1988; Geuze *et al.*, 1989; Woods *et al.*, 1989). Dissociation of lysosomal enzymes is known to be triggered by low pH, i.e., ~5.5. Herein we describe another case of a receptor that can recycle from the late endosome compartment and escape lysosomal degradation. Interestingly, it does so when trafficking with bound RAP-GST but not when trafficking with bound ligand. Since RAP-GST is known to bind to all members of the LDL receptor gene family (Strickland *et al.*, 1991; Orlando *et al.*, 1992; Battey *et al.*, 1994; Medh *et al.*, 1995), it seems likely that the same itinerary applies when RAP-GST is bound to other LDL receptor family members.

Paucity of Knowledge on Endocytic Sorting and Trafficking Signals on Megalin

It is generally recognized that the signals for sorting of recycling endocytic receptors into clathrin-coated pits consist of short tyrosine-containing sequences in the cytoplasmic domain of the receptors that vary in amino acid sequence but share a common conformational determinant, a tight turn (Trowbridge *et al.*, 1993). These sequences allow selective uptake of macromolecules by interaction between the receptor tails and adaptor complexes that enhance the assembly of clathrin lattices (Pearse, 1988). The prototype of the tyrosine-containing signal is the (FX)NPXY of the LDL receptor (Goldstein *et al.*, 1985; Chen *et al.*, 1990). Megalin contains two such NPXY motifs in its cytoplasmic tail (Saito *et al.*, 1994), but it is not yet known whether one or both of these motifs is required for clustering in coated pits and internalization. The megalin cytoplasmic tail consists of 213 amino acids (versus 50 for the LDL receptor). Except for the NPXY sequences, the composition of the cytoplasmic tail of megalin is unique and shares no common features with other members of the LDL receptor family.

(Figure 10 cont.) ¹²⁵I-labeled LPL by 86 and 87%, respectively. (B) Distribution of ¹²⁵I-labeled LPL after uptake at 18°C for 1 h (□) or 18°C followed by 37°C for 15 min (■) detected by direct gamma counting. At 18°C, LPL sediments exclusively with the plasma membrane and early endosomes (fractions 1–4). After 5 min at 37°C, the majority of LPL is already present in lysosomes (fractions 10–12). (C) Distribution of ¹²⁵I-labeled megalin (labeled by cell surface iodination) in the same gradient fractions shown in B after incubation of L2 cells with ¹²⁵I-labeled LPL at 18°C (1 h) followed by 37°C (5 min). ¹²⁵I-labeled megalin (determined by immunoprecipitation with anti-megalin antibody) is present only in fractions 1–6 with the majority in fractions 3 and 4 (early endosomes). (D) Quantitation of the immunoprecipitation data shown in C.

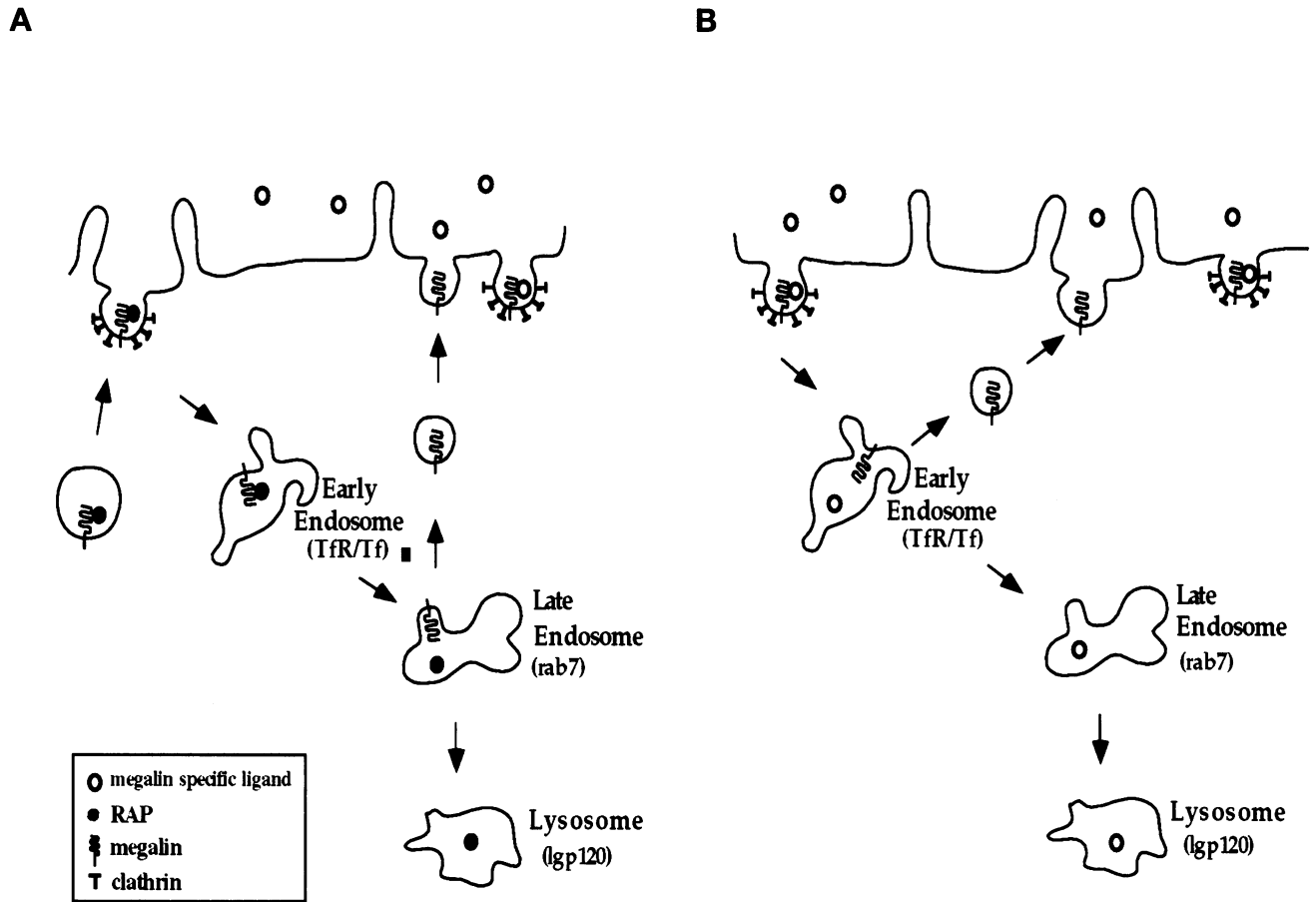


Figure 11. Model depicting the endocytic trafficking pathway of megalin/RAP complexes and megalin/ligand complexes. (A) Megalin/RAP complexes formed in the ER traffic to the cell surface. Since RAP competes for the binding of all known ligands to megalin, RAP must dissociate from megalin for the receptor to be capable of binding ligands. Our data suggest that megalin/RAP complexes at the cell surface are internalized via clathrin-coated pits and pass through early endosomes to late endosomes apparently by a pH-dependent mechanism. RAP is rapidly degraded in lysosomes, and megalin is recycled to the cell surface where it is utilized for ligand binding. (B) Newly formed megalin/ligand complexes are endocytosed and dissociate in early endosomes. Megalin is recycled, and the ligand is delivered to lysosomes and degraded.

Once endocytic receptors enter cells via coated pits, they are assumed to be processed through the same subset of endosomes. Moreover, studies on tailless mutants indicate that once receptors enter the pathway, they travel back to the cell surface constitutively without the need for further traffic information (Trowbridge *et al.*, 1993). Also, many receptors, such as the TfR and LDL receptor, constitutively recycle whether occupied or not. What could be responsible for the difference in the trafficking itinerary of megalin with bound ligand versus bound RAP? The simplest explanation is that dissociation of RAP requires a lower pH than dissociation of ligands. Thus, the megalin/RAP complexes continue down the endocytic pathway until they reach late endosomes where they find the lower pH milieu required for dissociation of RAP.

All members of the LDL receptor family share the same four motifs in their extracellular domains: the ligand binding, EGF, growth factor, and YWTD repeats. Megalin is known to have four clusters of ligand-binding repeats separated by YWTD spacer regions. The binding sites for several ligands (Orlando *et al.*, 1997) as well as for binding of pathogenic antibodies (Saito *et al.*, 1996) have been mapped to the fifth ligand-binding repeat (42 amino acids) in the second cluster of ligand-binding repeats. The binding site for RAP has not been directly demonstrated, but the fact that RAP-GST competes for ligand binding to megalin suggests that it binds to the same site. We are currently constructing truncated "minireceptors" whose extracellular domains are limited to the second cluster of ligand-binding repeats to study further the molecular mechanisms of megalin trafficking and ligand binding.

ACKNOWLEDGMENTS

We thank Drs. Fred Gage, Salk Institute, and Larry Goldstein, Howard Hughes Medical Institute, University of California San Diego, for the use of their Bio-Rad MRC 1000 confocal microscopes. This work was supported by National Institutes of Health grant DK-17724 to M.G.F. R.-P.C. was the recipient of a fellowship (AHA 93-59) from the California Division of the American Heart Association.

REFERENCES

- Batthey, F.D., Gafvels, M.E., FitzGerald, D.J., Argraves, W.S., Chappell, D.A., Strauss, J.F., III, and Strickland, D.K. (1994). The 39-kDa receptor-associated protein regulates ligand binding by the very low density lipoprotein receptor. *J. Biol. Chem.* **269**, 23268-23273.
- Biemersderfer, D., Dekan, G., Aronson, P., and Farquhar, M.G. (1993). Biosynthesis of the gp330/44-kDa Heymann nephritis antigenic complex: assembly takes place in the ER. *Am. J. Physiol.* **264**, F1011-F1020.
- Brown, M.S., Herz, J., Kowal, R.C., and Goldstein, J.L. (1991). The low density lipoprotein-related protein: double agent or decoy? *Curr. Opin. Lipidol.* **2**, 65-72.
- Brown, W.J., Goodhouse, J., and Farquhar, M.G. (1986). Mannose-6-phosphate receptors for lysosomal enzymes cycle between the Golgi complex and endosomes. *J. Cell Biol.* **103**, 1235-1247.
- Bu, G., Maksymovitch, E.A., Geuze, H., and Schwartz, A.L. (1994). Subcellular localization and endocytic function of low density lipoprotein receptor-related protein in human glioblastoma cells. *J. Biol. Chem.* **269**, 29874-29882.
- Bu, G., and Rennke, S. (1996). Receptor-associated protein is a folding chaperone for low density lipoprotein receptor-related protein. *J. Biol. Chem.* **271**, 22218-22224.
- Chen, W.-J., Goldstein, J.L., and Brown, M.S. (1990). NPXY, a sequence often found in cytoplasmic tails, is required for coated pit-mediated internalization of the low density lipoprotein receptor. *J. Biol. Chem.* **265**, 3116-3123.
- Christensen, E.I., Gliemann, J., and Moestrup, S.K. (1992). Renal tubule gp330 is a calcium binding receptor for endocytic uptake of protein. *J. Histochem. Cytochem.* **40**, 1481-1490.
- Czekay, R.-P., Orlando, R.A., Woodward, L., Adamson, E.D., and Farquhar, M.G. (1995a). The expression of megalin and LRP diverges in differentiating F9 embryonal carcinoma cells. *J. Cell Sci.* **108**, 1433-1441.
- Czekay, R.P., Orlando, R.A., Woodward, L., and Farquhar, M.G. (1995b). Megalin/RAP complexes taken up by endocytosis dissociate in late endosomes and megalin recycles to the cell surface. *Mol. Biol. Cell* **6**, 285a.
- Duncan, J.R., and Kornfeld, S. (1988). Intracellular movement of two mannose 6-phosphate receptors: return to the Golgi apparatus. *J. Cell Biol.* **106**, 617-628.
- Dunn, K.W., McGraw, T.E., and Maxfield, F.R. (1989). Iterative fractionation of recycling receptors from lysosomally destined ligands in an early sorting endosome. *J. Cell Biol.* **109**, 3303-3314.
- Farquhar, M.G., Kerjaschki, D., Lundstrom, M., and Orlando, R.A. (1994). Gp330 and RAP: the Heymann nephritis antigenic complex. *Ann. NY Acad. Sci.* **737**, 96-113.
- Farquhar, M.G., Saito, A., Kerjaschki, D., and Orlando, R.A. (1995). The Heymann nephritis antigenic complex: megalin (gp330) and RAP. *J. Am. Soc. Nephrol.* **6**, 35-47.
- Feng, Y., Press, B., and Wandinger-Ness, A. (1995). Rab 7: an important regulator of late endocytic membrane traffic. *J. Cell Biol.* **131**, 1435-1452.
- Galloway, C.J., Dean, G.E., Marsh, M., Rudnick, G., and Mellman, I. (1983). Acidification of macrophage and fibroblast endocytic vesicles in vitro. *Proc. Natl. Acad. Sci. USA* **80**, 3334-3338.
- Geuze, H.J., Stoorvogel, W., Strous, G.J., Slot, J.W., Zijderhand-Bleekemolen, J., and Mellman, I. (1989). Sorting of mannose-6-phosphate receptors and lysosomal membrane proteins in endocytic vesicles. *J. Cell Biol.* **107**, 2491-2501.
- Goldstein, J.L., Brown, M.S., Anderson, R.G.W., Russell, D.W., and Schneider, W.J. (1985). Receptor-mediated endocytosis: concepts emerging from the LDL receptor system. *Annu. Rev. Cell Biol.* **1**, 1-39.
- Griffiths, G., Hoflack, B., Simons, K., Mellman, I., and Kornfeld, S. (1988). The mannose-6-phosphate receptor and the biogenesis of lysosomes. *Cell*, **52**, 329-341.
- Hobman, T.C., Woodward, L., and Farquhar, M.G. (1992). The rubella virus E1 glycoprotein is arrested in a novel post-ER pre-Golgi compartment. *J. Cell Biol.* **118**, 795-812.
- Kerjaschki, D., and Farquhar, M.G. (1983). Immunocytochemical localization of the Heymann nephritis antigen (gp330) in glomerular epithelial cells of normal Lewis rats. *J. Exp. Med.* **157**, 667-686.
- Kerjaschki, D., Miettinen, A., and Farquhar, M.G. (1987). Initial events in the formation of immune deposits in passive Heymann nephritis: gp330-anti-gp330 immune complexes form in epithelial coated pits and rapidly become attached to the GBM. *J. Exp. Med.* **166**, 109-128.
- Kerjaschki, D., Ullrich, R., Exner, M., Orlando, R.A., and Farquhar, M.G. (1996). Induction of passive Heymann nephritis with antibodies specific for a synthetic peptide derived from the receptor-associated protein. *J. Exp. Med.* **183**, 2007-2015.
- Kornfeld, S., and Mellman, I. (1989). The biogenesis of lysosomes. *Annu. Rev. Cell Biol.* **5**, 483-525.
- Kounnas, M.Z., Argraves, W.S., and Strickland, D.K. (1992). The 39-kDa receptor-associated protein interacts with two members of the low density lipoprotein receptor family, alpha2-macroglobulin receptor and glycoprotein 330. *J. Biol. Chem.* **267**, 21162-21166.
- Kounnas, M.Z., Chappell, D.A., Strickland, D.K., and Argraves, W.S. (1993). Glycoprotein 330, a member of the low density lipoprotein receptor family, binds lipoprotein lipase in vitro. *J. Biol. Chem.* **268**, 14176-14181.
- Kounnas, M.Z., Stefansson, S., Loukinova, E., Argraves, K.M., Strickland, D.K., and Argraves, W.S. (1994). An overview of the structure and function of glycoprotein 330, a receptor related to the alpha2-macroglobulin receptor. *Ann. NY Acad. Sci.* **737**, 114-123.
- Krieger, M., and Herz, J. (1994). Structures and functions of multi-ligand lipoprotein receptors: macrophage scavenger receptors and LDL receptor-related protein (LRP). *Annu. Rev. Biochem.* **63**, 601-637.
- Laemmli, U.K. (1970). Cleavage of structural proteins during the assembly of the head of bacteriophage T₄. *Nature* **227**, 680-685.
- Lamaze, C., and Schmid, S.L. (1995). The emergence of clathrin-independent pinocytic pathways. *Curr. Opin. Cell Biol.* **7**, 573-580.
- Lundstrom, M., Orlando, R.A., Saedi, M.S., Woodward, L., Kurihara, H., and Farquhar, M.G. (1993). Immunocytochemical and biochemical characterization of the Heymann nephritis antigenic complex in rat L2 yolk sac cells. *Am. J. Pathol.* **143**, 1423-1435.
- McCaffery, M., and Farquhar, M.G. (1995). Localization of GTPases (GTP-binding proteins) by indirect immunofluorescence and immunoelectron microscopy. *Methods Enzymol.* **257**, 259-279.
- McLean, W., and Nakane, P.F. (1973). A new fixative for immunoelectron microscopy. *J. Histochem. Cytochem.* **22**, 1077-1083.

- Medh, J.D., Fry, G.L., Bowen, S.L., Pladet, M.W., Strickland, D.K., and Chappell, D.A. (1995). The 39-kDa receptor-associated protein modulates lipoprotein catabolism by binding to LDL receptors. *J. Biol. Chem.* 270, 536–540.
- Moestrup, S.K., Cui, S., Vorum, H., Bregengard, C., Bjorn, S.E., Norris, K., Gliemann, J., and Christensen, E.I. (1995). Evidence that epithelial glycoprotein 330/megalin mediates uptake of polybasic drugs. *J. Clin. Invest.* 96, 1404–1413.
- Moestrup, S.K., Nielsen, S., Andreasen, P., Jorgensen, K.E., Nykjaer, A., Roigaard, H., Gliemann, J., and Christensen, E.I. (1993). Epithelial glycoprotein-330 mediates endocytosis of plasminogen activator-plasminogen activator inhibitor type-1 complexes. *J. Biol. Chem.* 268, 16564–16570.
- Orlando, R.A., Exner, M., Czekay, R.-P., Yamazaki, H., Saito, A., Ullrich, R., Kerjaschki, D., and Farquhar, M.G. (1997). Identification of the second cluster of ligand binding repeats in megalin as a site for receptor-ligand interactions. *Proc. Natl. Acad. Sci. USA*, in press.
- Orlando, R.A., and Farquhar, M.G. (1993). Identification of a cell line that expresses a cell surface and a soluble form of the gp330/receptor-associated protein (RAP) Heymann nephritis antigenic complex. *Proc. Natl. Acad. Sci. USA* 90, 4082–4086.
- Orlando, R.A., and Farquhar, M.G. (1994a). Cellular trafficking of megalin (gp330) and the receptor associated protein (RAP). *Mol. Biol. Cell* 5, 187a.
- Orlando, R.A., and Farquhar, M.G. (1994b). Functional domains of the receptor-associated protein (RAP). *Proc. Natl. Acad. Sci. USA* 91, 3161–3165.
- Orlando, R.A., Kerjaschki, D., Kurihara, H., Biemesderfer, D., and Farquhar, M.G. (1992). Gp330 associates with a 44-kDa protein in the rat kidney to form the Heymann nephritis antigenic complex. *Proc. Natl. Acad. Sci. USA* 89, 6698–6702.
- Pearse, B.M. (1988). Receptors compete for adaptors found in plasma membrane coated pits. *EMBO J.* 7, 3331–3336.
- Raychowdhury, R., Niles, J.L., McCluskey, R.T., and Smith, J.A. (1989). Autoimmune target in Heymann nephritis is a glycoprotein with homology to the LDL receptor. *Science* 244, 1163–1165.
- Saito, A., Pietromonaco, S., Loo, A., and Farquhar, M.G. (1994). Complete cloning and sequencing of rat gp330/“megalin,” a distinctive member of the low density lipoprotein receptor gene family. *Proc. Natl. Acad. Sci. USA* 91, 9725–9729.
- Saito, A., Yamazaki, H., Rader, K., Nakatani, A., Ullrich, R., Kerjaschki, D., Orlando, R.A., and Farquhar, M.G. (1996). Mapping rat megalin: the second cluster of ligand binding repeats contains a 46-amino acid pathogenic epitope involved in the formation of immune deposits in Heymann nephritis. *Proc. Natl. Acad. Sci. USA* 93, 8601–8605.
- Strickland, D.K., Ashcom, J.D., Williams, S., Battey, F., Behre, E., McTigue, K., Battey, J.F., and Argraves, W.S. (1991). Primary structure of α_2 -macroglobulin receptor-associated protein: human homologue of a Heymann nephritis antigen. *J. Biol. Chem.* 266, 13364–13369.
- Trowbridge, I.S., Collawn, J.F., and Hopkins, C.R. (1993). Signal-dependent membrane protein trafficking in the endocytic pathway. *Annu. Rev. Cell Biol.* 9, 129–161.
- Williams, S.E., Ashcom, J.D., Argraves, W.S., and Strickland, D.K. (1992). A novel mechanism for controlling the activity of α_2 -macroglobulin receptor/low density lipoprotein receptor-related protein. *J. Biol. Chem.* 267, 9035–9040.
- Willnow, T.E., Goldstein, J.L., Orth, K., Brown, M.S., and Herz, J. (1992). Low density lipoprotein receptor-related protein and gp330 bind similar ligands, including plasminogen activator-inhibitor complexes and lactoferrin, an inhibitor of chylomicron remnant clearance. *J. Biol. Chem.* 267, 26172–26180.
- Willnow, T.E., Rohlmann, A., Horton, J., Otani, H., Braun, J.R., Hammer, R.E., and Herz, J. (1996). RAP, a specialized chaperone, prevents ligand-induced ER retention and degradation of LDL receptor-related endocytic receptors. *EMBO J.* 15, 2632–2639.
- Woods, J.W., Goodhouse, J., and Farquhar, M.G. (1989). Transferrin receptors and cation independent mannose-6-phosphate receptors deliver their ligands to two distinct subpopulations of multivesicular endosomes. *Eur. J. Cell Biol.* 50, 132–143.
- Yamamoto, K., Katsuda, N., Himeno, M., and Kato, K. (1979). Cathepsin D of rat spleen: affinity purification and properties of two types of cathepsin D. *Eur. J. Biochem.* 95, 459–67.
- Yamashiro, D.J., and Maxfield, F.R. (1984). Acidification of endocytic compartments and the intracellular pathways of ligands and receptors. *J. Cell. Biochem.* 26, 231–46. 1